Chin. Geogra. Sci. 2011 21(3) 322–333
doi: 10.1007/s11769-011-0472-2
www.springerlink.com/content/1002-0063

Crop Classification Using MODIS NDVI Data Denoised by Wavelet: A Case Study in Hebei Plain, China

ZHANG Shengwei[1, 2], LEI Yuping[2], WANG Liping[1], LI Hongjun[2], ZHAO Hongbin[1]
(*1. Inner Mongolia Agricultural University, Hohhot 010018, China; 2. Center for Agricultural Resources Research, Institute of Genetics and Developmental Biology, Chinese Academy of Sciences, Shijiazhuang 050021, China*)

Abstract: Time-series Moderate Resolution Imaging Spectroradiometer (MODIS) Normalized Difference Vegetation Index (NDVI) data have been widely used for large area crop mapping. However, the temporal crop signatures generated from these data were always accompanied by noise. In this study, a denoising method combined with Time series Inverse Distance Weighted (T-IDW) interpolating and Discrete Wavelet Transform (DWT) was presented. The detail crop planting patterns in Hebei Plain, China were classified using denoised time-series MODIS NDVI data at 250 m resolution. The denoising approach improved original MODIS NDVI product significantly in several periods, which may affect the accuracy of classification. The MODIS NDVI-derived crop map of the Hebei Plain achieved satisfactory classification accuracies through validation with field observation, statistical data and high resolution image. The field investigation accuracy was 85% at pixel level. At county-level, for winter wheat, there is relatively more significant correlation between the estimated area derived from satellite data with noise reduction and the statistical area (R^2 = 0.814, $p < 0.01$). Moreover, the MODIS-derived crop patterns were highly consistent with the map generated by high resolution Landsat image in the same period. The overall accuracy achieved 91.01%. The results indicate that the method combining T-IDW and DWT can provide a gain in time-series MODIS NDVI data noise reduction and crop classification.

Keywords: remote sensing imagery; Moderate Resolution Imaging Spectroradiometer (MODIS); Normalized Difference Vegetation Index (NDVI); noise reduction; crop land classification

Citation: Zhang Shengwei, Lei Yuping, Wang Liping, Li Hongjun, Zhao Hongbin, 2011. Crop classification using MODIS NDVI data denoised by wavelet: A case study in Hebei Plain, China. *Chinese Geographical Science*, 21(3): 322–333. doi: 10.1007/s11769-011-0472-2

1 Introduction

The satellite-based remote sensing data have been widely applied to providing a cost-effective way to develop large geographic regional land use/land cover (LULC) classification. Over the past decade, the science of large-area LULC mapping had made significant progress as the same as improved remotely sensed data and computing resources, and advanced classification techniques. Numerous efforts devoted into large-area LULC mapping at regional (Homer *et al.*, 2004; Wessels *et al.*, 2004) and global (Friedl *et al.*, 2002; Bartholome and Belward, 2005) scale have been known through literatures. However, little attention has been paid to large-area crop mapping and monitoring. Most of the highlights of mapping efforts focused on the classification of land cover types associated with natural systems (e.g., forest land, grassland, and shrubland) and have tended to generalize cropland areas into a single or limited number of thematic classes (Wardlow and Egbert, 2008). Few researches on large-area mapping attempted to map specific crop types and crop land transformation (Wardlow *et al.*, 2007; Galford *et al.*, 2008; Zhang *et al.*, 2008). It is known that the classification map is essential to assess the cropland changes which commonly occur every year. Especially in the irrigated agricultural regions in semi-

Received date: 2010-08-26; accepted date: 2011-03-01
Foundation item: Under the auspices of Knowledge Innovation Programs of Chinese Academy of Sciences (No. KZCX2-YW-449, KSCX-YW-09), National Natural Science Foundation of China (No. 40971025, 40901030, 50969003)
Corresponding author: LEI Yuping. E-mail: leiyp@sjziam.ac.cn

arid area, the cropland pattern is a significant factor for agricultural water management. Thus, an accurate and timely mapping methodology is necessary to characterize the regional-scale cropping pattern and to provide improved LULC information to scientists and policy makers. However, the development of a large-area crop mapping methodology is complicated because it requires remotely sensed data which have large geographic coverage, high temporal resolution, adequate spatial resolution, minimal cost and is easy to implement, if possible.

Moderate Resolution Imaging Spectroradiometer (MODIS) data products offer a great opportunity for land-cover and land-use change studies due to their characteristics of moderate spatial resolution, frequent observations, enhanced spectral resolution and improved atmospheric calibration (Zhang *et al.*, 2003) and being free to the end user. Moreover, the MODIS Land Science Team provides a suite of standard MODIS data products to users, including 16-day composited MODIS 250 m Vegetation Index (VI) product (MOD13Q1) and yearly MODIS land cover products (MOD12). However, the current 1-km MODIS global land cover classification resolution may be too coarse for local application.

In an analysis of the MODIS VI product data for more than 2000 fields in Kansas, the data were found to have sufficient spatial, spectral, temporal, and radiometric resolutions to detect unique multi-temporal VI signatures for the state's major crop types and land use practices (Wardlow *et al.*, 2007). Time-series Normalized Difference Vegetation Index (NDVI) data can distinguish different vegetation characteristics through acquiring the unique value at individual phase during plant growth period (Boles *et al.*, 2004). Many researches had been carried out using time-series NDVI data to classify land-cover map (Friedl *et al.*, 2002) and to monitor vegetation dynamics (Sakamoto *et al.*, 2005; Lunetta *et al.*, 2006). However, time-series data are often affected by various noise components such as cloud presence, atmospheric variability, aerosol scattering and bi-directional effects (Xiao *et al.*, 2003; Sakamoto *et al.*, 2005). Such time-series data from remote sensing may have unpredicted noise, which will limit the use of traditional classification methods based on statistical assumptions. Thus, noise reduction or filter processing is necessary before the time-series NDVI data are used for further analyses (Xiao *et al.*, 2003; Lunetta *et al.*, 2006). There were many methods and tools for such preprocessing including Best Index Slope Extraction (BISE) (Viovy *et al.*, 1992) and modified BISE (Lovell and Graetz, 2001), Asymmetric Gaussian (AG) technique (Jönsson and Eklundh, 2002), Savitzky-Golay (Savitzky and Golay, 1964) and modified Savitzky-Golay (Chen *et al*., 2004), fast Fourier transform technique and others Fourier-based fitting methods (Sellers *et al*., 1994; Roerink *et al.*, 2000; Zhang *et al.*, 2008), mean-value iteration (MVI) filter (Ma and Veroustraete, 2006), double logistic function-fitting (Beck *et al.*, 2006), and wavelet transform method (Galford *et al.*, 2008), and currently, Julien and Sobrino (2010) presented the iterative Interpolation for Data Reconstruction (IDR) method.

Many different methods were compared in previous researches, such as AG function and BISE, AG function and Fourier-based method (Jönsson and Eklundh, 2002), modified Savitzky–Golay and fast Fourier transform (Chen *et al*., 2004). Hird and Mcdermid (2009) preformed quantitative assessments of six different noise reduction methods. The results indicate that each method has its advantages and drawbacks which limit its application (Jönsson and Eklundh, 2002; Chen *et al.*, 2004). At present, the researches on noise-reduction are mostly focused on the outliers of time-series NDVI. However, the method keeping the high quality NDVI values is ignored. In addition, little attention has been paid to the application effect of noise reduced time-series NDVI, such as the result of the regional classification derived from the noise reduced NDVI.

The objective of this study is to map the crop pattern in the Hebei Plain which is one of the major grain-producing areas of China. Meanwhile, investigating the applicability and accuracy of time-series MODIS NDVI data denoised by Time series Inverse Distance Weighted interpolating (T-IDW) and wavelet for crop classification at regional scale were also implemented. The classification map of different crop types was validated by both statistical data and fine-resolution remote sensing data to evaluate the noise reduction and the classification method.

2 Study Area and Data

2.1 Study area

In this study, the Hebei Plain, with an area of 62 020 km^2, is selected as the study area which is consisted of 83 counties (Fig. 1). In this area, agriculture is the largest water consumer. Meanwhile, rapid economic develop-

ment and population growth are increasing pressure on water supplies. The shortage of water resources has become a serious restraining factor for the development of this area (Liu *et al.*, 2001). In the study area, 72% of the total area is cultivated land, and the major crop types are winter wheat (*Triticum aestivum* L.) and summer maize (*Zea mays* L.). The growing season of winter wheat is from early October to mid-June next year, and summer maize is nurtured at the end of winter wheat growth season and harvested in last September. Cotton (*Gossypium* spp.) and spring maize (*Zea mays* L.) are also planted in this area with the growing season from mid-April to mid-October. The climate is temperate semi-arid with a strong summer monsoon season. Average monthly temperature ranges from about –2.5℃ in January to 26℃ in July, with an average annual temperature of about 13.2℃ and annual frost free days about 150–210 days. The average annual precipitation is about 400–500 mm, of which about 70% is concentrated in July–September.

2.2 MODIS NDVI 16-day composited data

MODIS NDVI 16-day composite grid data (MOD13Q1) are provided every 16 days at 250 m spatial resolution as a gridded level-3 product in the Sinusoidal projection (Huete *et al.*, 1999). In version 005 a new compositing scheme is utilized, which reduces angular, sun-target-sensor variations, using the Constrained View Maximum Value Composite (CV-MVC) and an option to use BRDF models (Didan and Huete, 2006). MOD13Q1 file in Hierarchical Data Format-Earth Observing System (HDF-EOS) format was acquired from January to December 2006 from the Land Processes Distributed Active Archive Center of U.S. Geological Survey (USGS LP DACC) data pool (USGS, 2009). Detailed documents on MODIS NDVI compositing process and Quality Assessment Science Data Sets (QASDS) can be found at MODIS Vegetation Index (MOD13) Algorithm Theoretical Basis Document (Huete *et al.*, 1999).

2.3 Validation data set

Accuracy assessment of land cover products from coarse-resolution satellite dataset is a critical and challenging task, because these maps can over or underestimate cover types due to the fragmentation and sub-pixel proportion of each cover type (Achard and Mayaux, 2001). As an alternative approach, land cover maps derived from fine-resolution images have been used for

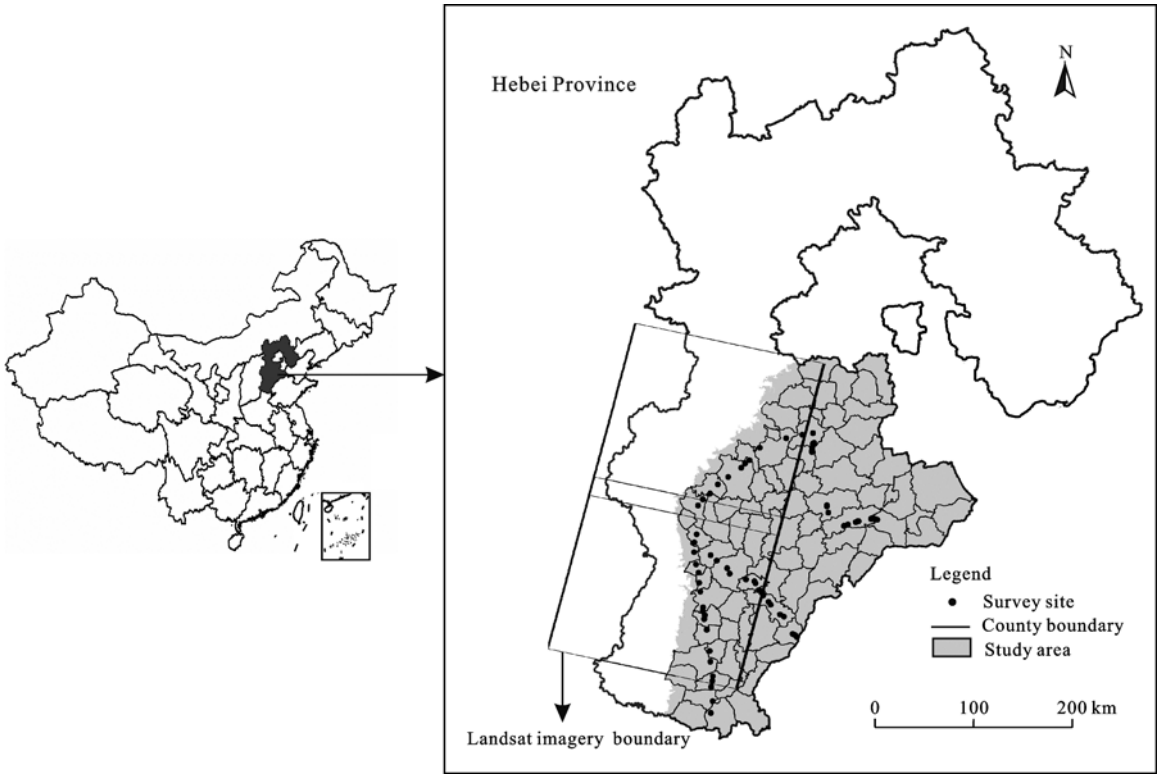

Fig. 1 Location of study area and survey sites

coarse-resolution classification map validation (Lotsch *et al.*, 003; Wu *et al.*, 2008). In this study, both statistical data and fine-resolution Landsat data derived classification map were used to validate the MODIS-derived crop area. The statistical data was gathered from Rural Statistical Yearbook of Hebei Province (Cao *et al.*, 2007). Two Landsat imageries in September 5, 2006 were obtained from International Scientific & Technical Data Mirror Server of Chinese Academy of Sciences. The path of these two Landsat imageries is 124 and the rows are 33 and 34, and the cover area is showed in Fig. 1.

Moreover, Magellan EX plorist 600 hand-held GPS receivers were used for the ground survey in 2006 and a set of 74 sites were sampled (Fig. 1), every site was about 1 km^2 with only one type of crop. The data of 40 survey sites were regarded as training sample used to generate dynamic NDVI time-series curve, and those of other survey sites for result evaluation.

3 Methodology

3.1 Data pre-processing

A time series of 16-day composite MODIS 250 m NDVI dataset spanning one growing season (January to December, 2006) were created for this study. Totally, 23 sets of 16-day composite MOD13Q1 data constituted the time series, and four tiles (h26v04, h26v05, h27v05 and h27v05) of the MODIS product were required for the whole study area coverage. For each composite period, the NDVI data were extracted from those MODIS vegetation indexes images. It was then mosaicked, and reprojected from the Sinusoidal to the UTM WGS-84 projection using a nearest neighbor resampling routine. Finally, the time-series dataset was subsetted to the study area boundary and multilayer image stack was developed for both the original NDVI data and Quality Assessment Science Data Set (QASDS).

3.2 Creating a T-IDW and wavelet denoised NDVI time series

In this study, a filter procedure composed of two steps was developed to generate high quality time-series signal. The first step is T-IDW interpolation based on NDVI Quality Assessment (QA) flags, and the second step is noise reduction by wavelet transformation. A wavelet-based method is used to remove the contaminated data in time-series MODIS NDVI data, because the wavelet transformation retains time components when transforming time-series data, and so can reproduce seasonal changes of vegetation without losing the temporal characteristics (Sakamoto *et al.*, 2005). The NDVI data stack is firstly filtered using QASDS ratings to remove poor-quality data values by T-IDW method. Those NDVI pixels corresponded to QASDS data quality rated as ′acceptable′ or higher are retained. Other pixels with ′bad′ quality ratings are flagged for interpolation. The T-IDW interpolation method can be expressed as Equation (1):

$$F(x, y, t) = \sum_{m=1}^{M} g(x, y, m) f(x, y, m) \quad (1)$$

where x, y is the location of ′bad′ flagged pixel, t is the period, $F(x, y, t)$ is the estimated value at time t, $f(x, y, m)$ is the value of adjacent pixel of time m, $g(x, y, m)$ is the weight of $f(x, y, m)$, and m is the maximum of the time distance.

The NDVI of crop changes continuously with the phenology in the real world. However, the period of MOD13 composited was 16 days. The interpolated value of NDVI will be significantly deviated if the time distance is set unreasonable. Therefore, considering both the phenology and MODIS composited period, the maximum of m is set as 2, which means that the NDVI values in one month taking effect in interpolation procedure.

Concretely, let $F(x, y, t)$ be the NDVI value for pixel (x, y) and composite t (varying from 1 to 23 in a year). For a ′bad′ flagged pixel in a composite time t, if all the pixels in $t + 1$, $t + 2$, $t - 1$, $t - 2$ are ′acceptable′, the $F(x, y, t)$ will be calculated as Equation (2):

$$F(x, y, t) = a_1 f(x, y, t-2) + a_2 f(x, y, t-1) + a_3 f(x, y, t+1) + a_4 f(x, y, t+2) \quad (2)$$

where a_1, a_2, a_3 and a_4 are weight parameters.

If the $f(x, y, t - 1)$ or the $f(x, y, t + 1)$ is ′bad′ flagged, then the $g(x, y, m)$ will change, and the $F(x, y, t)$ will be calculated as Equation (3):

$$F(x, y, t) = a_1 f(x, y, t-2) + a_2 f(x, y, t \pm 1) + a_3 f(x, y, t+2) \quad (3)$$

Although most of noise has been reduced by the first step mentioned above, some residual noise also remains because of the intense changes in the land surface. The

residual noise shows small fluctuation but higher than natural surface change in time-series in frequency. Therefore, a further noise reduction step was performed by employing Discrete Wavelet Transform (DWT).

Wavelet functions are a group of functions with oscillating and fast-decaying characteristics, which are generated from a mother wavelet by dilations and translations. The wavelet function is defined by Equation (4):

$$\psi_{a,b}(T)=\frac{1}{\sqrt{a}}\psi\left(\frac{T-b}{a}\right) \tag{4}$$

where a is the dilation or scaling parameter, and b is the translation or position parameter (Addison, 2002).

Wavelet analysis can accurately capture the local characteristics of non-stationary signals because it compacts support and fast-decaying. It means that the function′s duration was very limited and the time components of time-series data can be maintained during wavelet transformation.

The wavelet transformation $Wf(a, b)$ was defined by Equation (5):

$$Wf(a,b)=\frac{1}{\sqrt{a}}\int_{-\infty}^{+\infty}f(T)\psi\left(\frac{T-b}{a}\right)\mathrm{d}T \tag{5}$$

where $f(T)$ is the input signal, ψ is a mother wavelet, a is the dilation or scaling parameter, b is the translation or position parameter, and T represents the time-step in the one-dimensional time series over which the integration is performed (Addison, 2002).

The form of Equation (5) describes a wavelet transformation decomposed signal at various scales and shifts. The wavelet transformation can decompose both large-scale and small-scale components of a signal. The large-scale component represents the low frequency parts of the original signal or optimal approximations, and the small-scale component represents the high frequency parts of the original signal or detailed information (Lu *et al.*, 2007).

There are lots of redundancy signals in the continuous transformation instance. The redundancy signals would be useful in data reconstruction or feature extraction, but it will take too much computing time. For most practical applications, the DWT is accurate enough and can reconstruct signals perfectly (Mallat, 1989). The DWT analyzes signals over a discrete set of scales usually sampled at dyadic sequence. In discrete form the parameters a and b are given as follows:

$$(a,\ b)\ =\ (2^j,\ 2^jk) \tag{6}$$

where j and k are integers.

The dyadic form wavelet function is given as (Addison, 2002):

$$\psi_{j,k}(T)=2^{\frac{-j}{2}}\psi(2^{-j}T-k) \tag{7}$$

Applying the wavelet to a time series signal needs to select mother wavelet. The relevant parameters of mother wavelet include order and power by which the wavelet behavior is defined. A number of different mother wavelets existed, including daubechies family (dbN), derivative of a Gaussian (DOG) family and Coiflet family (Torrence and Compo, 1998). In this study, Coiflet mother wavelet with order 4 was used because the wavelet shape was as small as possible to match the peaks of NDVI value in agricultural phenology. A power threshold was required by wavelet noise removing processing. The power threshold corresponded to the number of coefficients determining how much of the input NDVI time series signal was retained. Error analysis was performed with the 70%, 80%, 90% and 95% power threshold. Observed NDVI data of cotton and winter wheat-summer maize were compared with 20 randomly selected sites with corresponding crop type. Average relative error (ARE, it is average value of all relative error of observed and wavelet transformed NDVI), R^2 and root mean square error (RMSE) were used in error analysis.

3.3 Classification method

The phenological characteristics (e.g. germination, vegetative phase, ripening, and harvest) of crop are reflected at the pixel-level in the time-series NDVI data. So in this study a knowledge-based land use classification model that combined remote sensing and phenological rules of crops in hierarchical decision tree was developed. The most important issue of this approach was the expert information of different crops on the seasonal phenological development in the study area. The average multi-temporal NDVI profiles and phenology of main crop types in the study area were generated from 40 sites among all the 74 sites.

Figure 2 shows the hierarchical classification tree which is composed of four levels and used in this study. At the first stage, the whole study area was mapped into vegetation and non-vegetation classes. Secondly, the

vegetation land areas were mapped into crop and non-crop. Then the crop areas could be separated into bi-modal crop (winter wheat-summer maize) and spring crop. The final step was to classify the spring crop into two specific types, spring maize and cotton. All the NDVI values in this step were multiplied by 10 000 to improve the speed of operation and storage.

3.4 Accuracy assessment

In order to assess the crop map derived from denoised time-series NDVI data, accuracy assessment of three different spatial levels was carried out in this study. The three spatial scales were pixel-level, county-level and regional-level. The pixel-level accuracy was performed by comparing time-series NDVI derived map with survey sites. At the county-level, the crops areas derived from satellite imagery were compared with the statistical data obtained from the Chinese Ministry of Agriculture Database. The regional-level accuracy was assessed by comparing the classification map derived from MODIS NDVI data and the high resolution Landsat data.

4 Results

4.1 Comparative analysis of denoising methods

Different power threshold (70%, 80%, 90% and 95%) effect on wavelet noise removing processing was presented in Table 1. The results show that the 90% power threshold has the maximum R^2 and minimum RMSE both in cotton and winter wheat-summer maize.

An example of comparison of various power threshold values for two crop types including cotton and winter wheat-summer maize double-cropping system is provided (Fig. 3). The 90% power threshold captures the overall data trend well, and gets closest to both high and low observed NDVI values. As Fig. 3 and Table 1 shown, the peaks of NDVI values under the 90% power

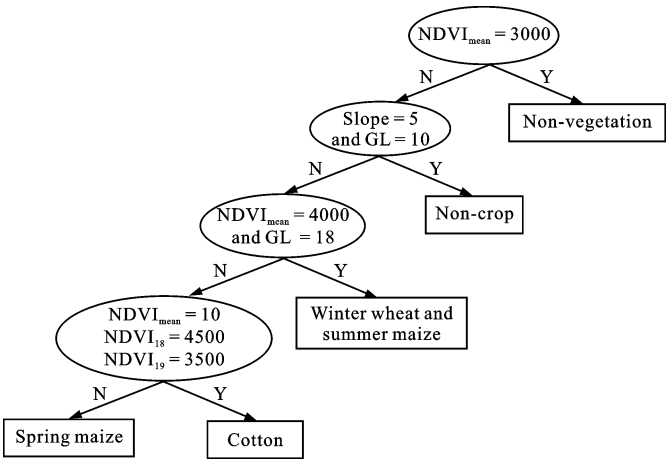

NDVI$_{mean}$: mean annual NDVI; Slope: topographic slope estimated from DEM data; GL: growth season length of vegetation calculated from period number of NDVI value higher than 3000; and NDVI$_{18}$ and NDVI$_{19}$ are NDVI values on September 30 and October 16, respectively

Fig. 2 Classification decision tree for discriminate different land covers based on time-series NDVI profile

Table 1 Error analysis of wavelet power threshold on timer-series NDVI data

Power threshold (%)	Crop type	ARE (%)	R^2	RMSE
95	Cotton	17.16	0.937	0.157
	Winter wheat-summer maize	16.22	0.900	0.153
90	Cotton	10.73	0.979	0.097
	Winter wheat-summer maize	13.79	0.924	0.132
80	Cotton	20.38	0.908	0.209
	Winter wheat-summer maize	16.53	0.884	0.161
70	Cotton	24.82	0.891	0.205
	Winter wheat-summer maize	20.24	0.775	0.224

Notes: ARE: average relative error; RMSE: root mean square error

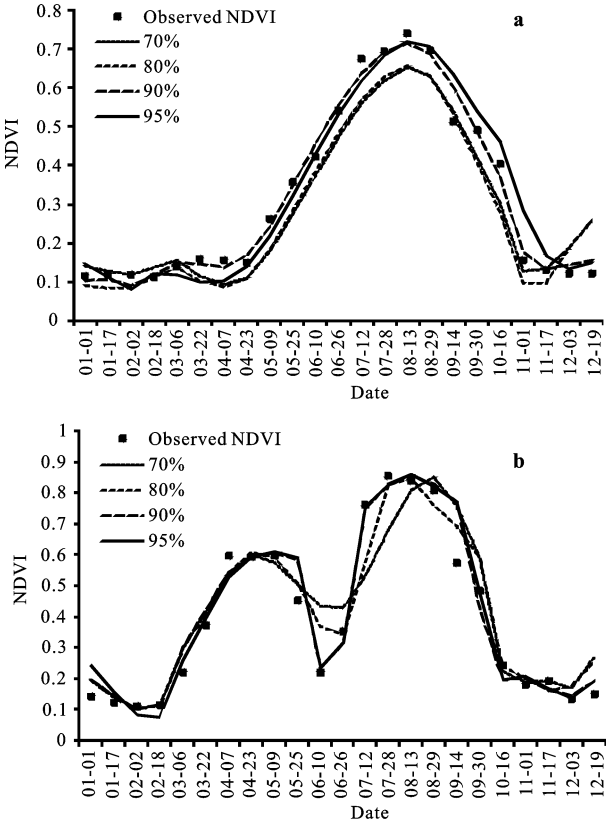

Fig. 3 Comparison of different wavelet-smoothed time-series values and observed NDVI of cotton (a) and winter wheat-summer maize double-cropping system (b) in 2006

threshold are removed effectively, although the double-cropping system makes the agricultural system more complex.

Assessment of the denoising effects between the original signals and denoised NDVI values by T-IDW, DWT and T-IDW combined with DWT were carried out for two primary crop types in the study area at pixel level. The winter wheat-summer maize double-cropping system and cotton were located at Luancheng Agro-Ecosystem Experimental Station, Chinese Academy of Sciences and Nangong County, respectively.

In Fig. 4, those NDVI values were from single pixel selected randomly in the study area, ang it demonstrates the reconstructed time-series NDVI for the crop types of cotton and winter wheat-summer maize. From Fig. 4a, it can be found that the T-IDW method based on QASDSA can remove a large amount of noise in the time series because almost all the noise is from abnormal peaks and troughs which have flagged in QASDSA. However, there is still some residual noise remained as little fluctuation. The DWT with Coiflet mother wavelet in order 4 and 90% wavelet power can remove some little fluctuation but have on power for those large peaks. The power should be changed to 68% to remove the large peak in selected cotton time-series NDVI data. However, a lower power, or fewer coefficients, retains less high frequency data by applying a wider wavelet which may capture trends through the entire time series but may lose phonological detail during a single year. By contrast, the method combined two steps including T-IDW and DWT performed much better than individual performance of T-IDW and DWT, since it can remove noise shown as abrupt rises or drops and unreasonable peak value and at the same time remain the right observations near the contaminated sites. The Fourier transform method was used as a comparison in this study, which can obtain better effort than T-IDW or DWT but it is

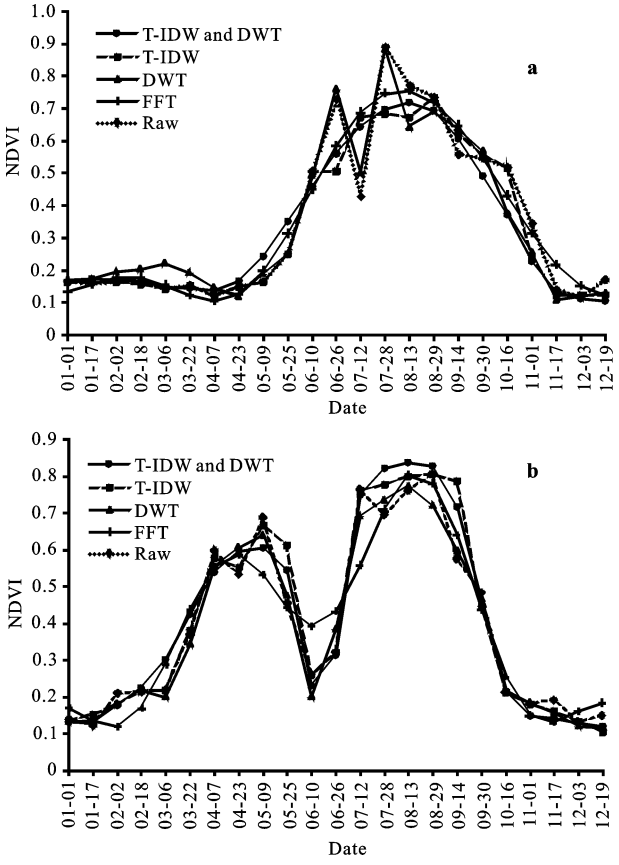

Raw is original signals; T-IDW is noise removed NDVI only by T-IDW method based on QASDSA; DWT is denoised NDVI only by DWT with Coiflet mother wavelet in order 4 and 90% power; FFT is noise removed NDVI by fast Fourier transform method (Zhang *et al*., 2008); and T-IDW and DWT means NDVI denoised by combined method with the same parameter as T-IDW and DWT

Fig. 4 Pixel multi-temporal NDVI profiles of cotton (a) and winter wheat-summer maize (b) denoised by different methods

similar with combined method. Figure 4b shows the noise reduction effect for bimodal crop. The situation of T-IDW, DWT and combined method are the same as mentioned above though the double cropping system contains more narrow peaks. However, the Fourier transform method was worse than combined method.

4.2 Crop classification

The major crops NDVI profile characteristics are consistent with the distinctive calendar of crops as shown in Fig. 5. The winter wheat is generally sown and then emerges in early October; initial tillering is witnessed at the beginning of November. The crop turns into dormant during the whole winter (December, January and February). Low NDVI values (0.25–0.35) from November through mid-March reflect this initial growth stage. In mid-March the winter wheat recovers and resumes growth in early spring when the air and soil temperatures get warm. This stage is represented by the rapid increase of NDVI values till mid-May which is the flowering stage of winter wheat. The ripening and senescence phase of winter wheat occur in late May and June and harvesting typically occurs during the first 10 days of June, expressed by the rapid decrease of NDVI values from 0.6 to 0.3 during this period. Summer maize is interplanted manually to winter wheat 5–7 days before harvest to prolong the growth period, reaching its utmost luxuriance in mid-August and then following with harvest at the end of September. At the beginning of October, land is plowed to prepare for winter wheat planting, and the two-crop rotation is repeated. So the bimodal signal is generated and acted as the fundamental basis of winter wheat-summer maize double cropping system classification.

Winter wheat-summer maize was relatively easily extracted because of the bimodal signal. On the contrary, the spring crops are difficult to discriminate because the unimodal signals are similar. Cotton and spring maize are both categorized as spring crop because the seedtime is in spring, and these crops almost have the same crop calendars. However, unique spectral-temporal responses that represent subtle differences in their growth cycle are reflected in timer-series NDVI profile.

Generally, differences in the planting date which is depicted by the different timings of their initial greenup are used to detect crop types among the spring crops. However, in this study the major spring crops of cotton and spring maize are almost sown at the same time in early May as shown in Fig. 5. It was difficult to distinguish the greenup time between these spring crops. Therefore, further analysis was performed to find out the variation in timing and value in these NDVI profiles, which are represented as different amplitude and phase in time-series signal. These differences were used as the basis of classification among these spring crops. As shown in Fig. 5, the spring maize peaked at July 28 with the highest NDVI value of 0.78. By contrast, the cotton peaked at August 13 with lower NDVI value of 0.72. The differences in crop type and canopy structure of spring maize and cotton could be represented by the NDVI values at peak growing season. In addition to the difference in peak growing season, the NDVI profiles of the two spring crops also exhibit different behaviors during the senescence stage. The large NDVI decrease at late July (July 28 composite period) represented the onset of the senescence of spring maize and this course continued until early October when harvest was executed and the NDVI values reached the lowest in this

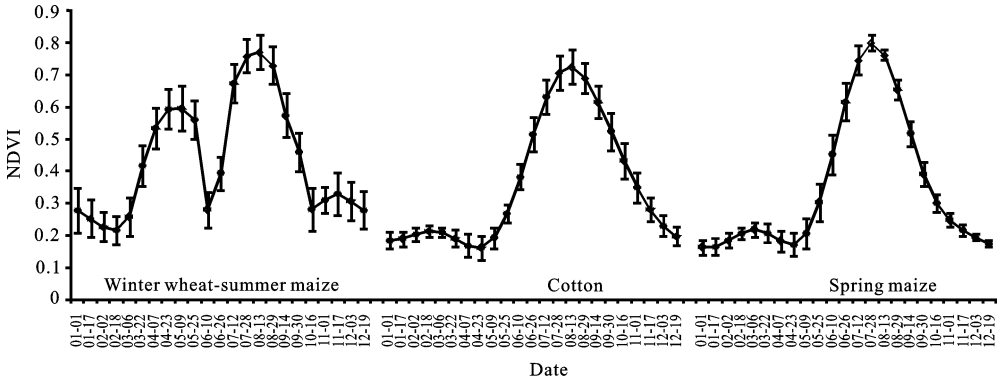

Fig. 5 Multi-temporal NDVI profiles of main crop categories in Hebei Plain

stage. Cotton exhibits a smooth NDVI decease curve, gradually from August 13 to November 17 composite periods, which reflects the extended period to dry the cotton balls and pick in batch.

Following the method of processing and classification, the classification map derived from time-series MODIS NDVI data is derived and shown in Fig. 6a. The spatial distribution of major crop and non-crop in the time-series NDVI derived map is consistent with the general land cover patterns of Hebei Plain. Main crop areas, such as the southeast and northeast cotton producing area, and large winter wheat-summer maize cropland, have been found to expand throughout the piedmont alluvial plain of the Taihang Mountains which is located in the west of the study area. The smaller and fragmented crop patches throughout the eastern coastal plains are also mapped. The patterns of the whole area in the general crop map are consistent with the cropping distribution (Cao *et al.*, 2007). The winter wheat-summer maize double-cropping system is dominant throughout the western and central plain. The spring crop class is mainly distributed in the northeast and southeast plain. In the southeast the cotton is the main crop, and in northeast the spring maize is planted widely corresponding to the cotton.

4.3 Classification assessment

In this study, accuracy assessment at pixel-level, county-level and regional-level were carried out for accurate and comprehensive evaluation. Firstly, at pixel-level, 34 remained survey sites were used to validate the MODIS derived classification results. There were 20 winter wheat-summer maize sites, nine cotton sites and five spring maize sites. The crop types in all the sites were correct with the corresponding classification results except for three winter wheat-summer corn sites, one cotton site and one spring maize site. The accuracy is 85% at pixel-level.

At county-level, the correlation between time-series MODIS-derived area and statistical area of the winter wheat is showed in Fig. 7. It can be observed that compared with raw NDVI values, the desonised NDVI values are closer to the statistical ones. There is relatively more significant correlation between the estimated area derived from satellite data with noise reduction and the statistical area ($R^2 = 0.814$, $p < 0.01$).

To validate the effect of noise reduction method in classification, a classification map with the same classifying parameters but without desnoising was derived (Fig. 6b). The area of winter wheat-summer maize and spring maize in Fig. 6b is obviously more than that in Fig. 6a. The spring maize area in the northeast is much larger, while the cotton area in the southeast is smaller and some areas of spring maize are found among the cotton field. NASA USGS land cover data is shown in Fig. 6c, in which the crop lands were treated as only one type. This is obviously inaccuracy either compared with survey data or statistical data.

Finally, the regional-level comparison was performed by comparing classification result with high-resolution Landsat image. Figure 8 shows the classification map derived from 250 m time-series MODIS NDVI data, 30

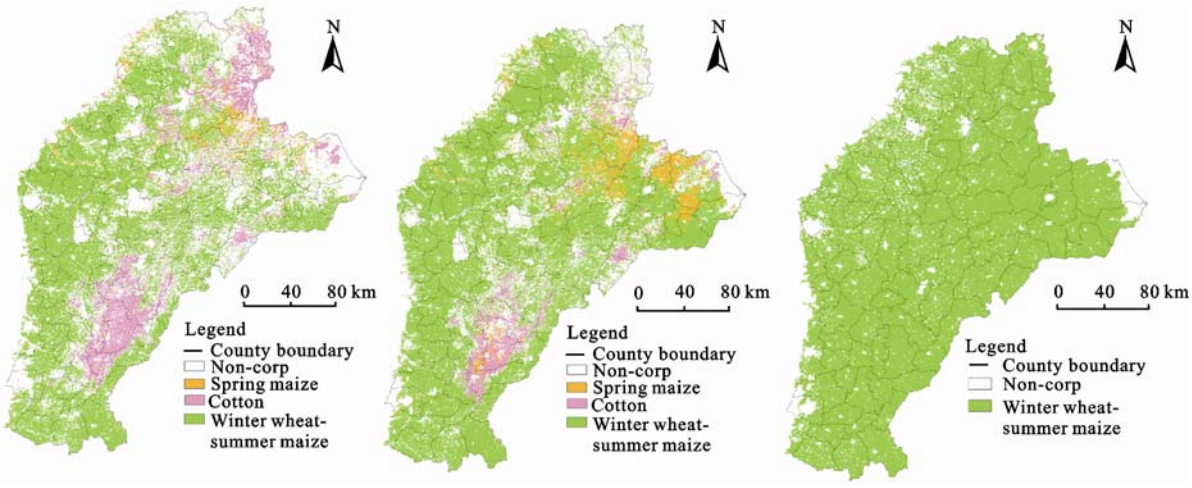

Fig. 6 Crop classification results of Hebei Plain from denoised NDVI data (a), raw NDVI data (b) and MCD12Q1 (MODIS land cover type product) (c)

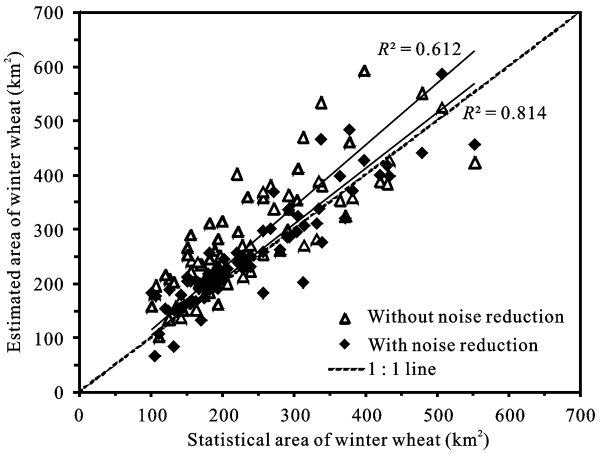

Fig. 7 A county-level comparison of winter wheat area from statistical data and derived from MODIS NDVI data with and without noise reduction

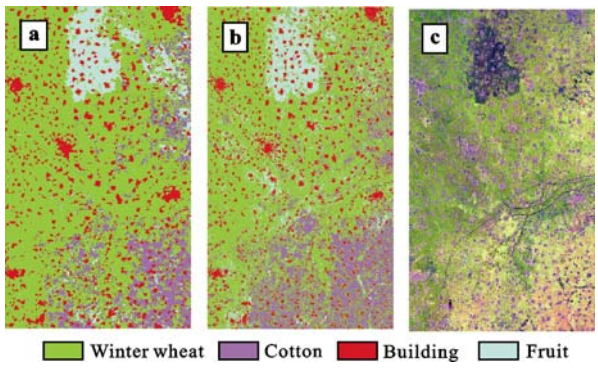

Fig. 8 Comparison of MODIS-derived 250 m general crop map (a), Landsat TM derived classification map (b), and false-color (RGB: band 5, band 4, and band 3) Landsat TM imagery (c) in central study area

m Landsat false-color TM imagery and Landsat TM derived classification map in the center of the study area. It indicates that the classified crop patterns in MODIS-erived map have a strong spatial correspondence to the cropping patterns in the Landsat TM imagery.

In addition, a confusion matrix (Chawla *et al.*, 2002) was used to compare classification results derived by MODIS with the ground truth data which generated from TM-derived land cover map classified by maximum likelihood method (Table 2). Only cotton and winter wheat were considered in the confusion matrix because they are the main crops in the center of study area (Fig. 8). From Table 2, it can be found that the producer′s accuracies of cotton and winter wheat are 90.76% and 98.48%, respectively. Overall accuracy is 91.01%, and the Kappa coefficient is 0.904.

Table 2 Producer′s and user′s accuracy confusion matrix of classification results

Class	Ground truth (%)		
	Cotton	Winter wheat	Total user′s accuracy
Unclassification	0.84	0	0.17
Cotton	90.76	1.52	19.86
Winter wheat	8.40	98.48	79.97
Total producer′s accuracy	100	100	100
Total (pixels)	319	660	979
Overall accuracy		91.01%	
Kappa coefficient		0.904	

5 Discussion and Conclusions

In this study, a noise reduction method combining T-IDW and DWT was applied to filtering the time-series MODIS NDVI data generated from 16-day composited MODIS 250 m NDVI product. Then the denoised time-series data were used to classify the crops in the Hebei Plain to discriminate bimodal winter wheat-summer maize rotation system and unimodal spring corp. The classification map was compared with survey sites, statistical data and fine-resolution remote sensing data. The results indicate that time-series MODIS 250 m NDVI data provide a viable option for regional-scale crop mapping in the Hebei Plain. The accuracy is 85% at pixel-level. While at county-level, the classified crop land areas are well correlated with statistical data, and the R^2 is 0.814 for the area of winter wheat. Classification map derived from desnoised data is more reasonable than the data without noise removing and NASA USGS land cover data. Compared with the land cover map derived from time-series NDVI data by Friedl *et al*. (2002) and Canisius *et al*. (2007) on global and China, the results of this study are better. The landscape cropping patterns in MODIS-derived crop map have a strong spatial correspondence to the cropping patterns that can be visually interpreted in the Landsat TM imagery. The confusion matrix between MODIS-derived and Landsat-derived classification show that the overall accuracy is 91.01% and Kappa coefficient is 0.904. However, overestimations and (or) underestimations are detected at both country-level and regional-level mainly due to the fragmentation and sub-pixel proportion. Therefore, sub-pixel unmixing methods, which have been applied to MODIS 250 m data for LULC characterization (Lobell and Asner, 2004), are recommended to be investi-

gated to improve the classification results.

The time-series noise reduction method was evaluated in this study beside the assessment of classification results. The results show that the T-IDW method can remove most of the noise in the time series but some residual noise remains because of fluctuations. The DWT can remove some small fluctuations but can not afford those large peaks unless a higher threshold is applied. The method combining T-IDW and DWT performs much better results, not only removing noise but also remaining the details of crop phenology. The noised reduction effect of Fourier-based method (Zhang *et al*., 2008) was almost the same with that of this study. However, the high quality NDVI values were kept reasonable with the method presented in this research.

This study presented the primary results of using time-series 16-day composited MODIS NDVI data in the Hebei Plain. Additional research activities should be performed on this basis. For example, numerous other variables could be directly derived from MOIDS data such as multi-spectral metrics. Other vegetation indexes such as enhanced vegetation index and shorter time interval data for instance 8-day composite MODIS product would be considered in the next step for more accurate classification. The mapping method should also be tested for more crop types in other geographical regions to determine the applicability. Moreover, area such as crop land dynamic, crop yield and agricultural water management could be benefited by the classification map produced in this study for more reliable decision making.

Acknowledgements

The authors would like to thank Luancheng Agro-Ecosystem Experimental Station, Chinese Academy of Sciences for providing the vegetation data.

References

Achard F E H, Mayaux P, 2001. Tropical forest mapping from coarse spatial resolution satellite data: Production and accuracy assessment issues. *International Journal of Remote Sensing*, 22(14): 2741–2762. doi: 10.1080/01431160120548

Addison P S, 2002. *The Illustrated Wavelet Transform Handbook*. Bristol: The Institute of Physics Publishing.

Bartholome E, Belward A, 2005. GLC2000: A new approach to global land cover mapping from Earth observation data. *International Journal of Remote Sensing*, 26(9): 1959–1977. doi: 10.1080/01431160412331291297

Beck P, Atzberer C, Høgda K *et al*., 2006. Improved monitoring of vegetation dynamics at very high latitudes: A new method using MODIS NDVI. *Remote Sensing of Environment*, 100(3): 321−334. doi: 10.1016/j.rse.2005.10.021

Boles S, Xiao X, Liu J *et al*., 2004. Land cover characterization of Temperate East Asia using multi-temporal VEGETATION sensor data. *Remote Sensing of Environment*, 90(4): 477–489. doi: 10.1016/j.rse.2004.01.016

Canisius F, Turral H, Molden D, 2007. Fourier analysis of historical NOAA time series data to estimate bimodal agriculture. *International Journal of Remote Sensing*, 28(24): 5503−5522. doi: 10.1080/01431160601086043

Cao Zhenguo, Yang Jingxiang, Zhao Wenhai, 2007. Rural Statistical Yearbook of Hebei Province. Beijing: China Statistics Press, 476–522. (in Chinese)

Chawla N, Bowyer K, Hall L *et al*., 2002. SMOTE: Synthetic minority over-sampling technique. *Journal of Artificial Intelligence Research*, 16: 321–357. doi: 10.1613/jair.953

Chen J, Jonsson P, Tamura M *et al*., 2004. A simple method for reconstructing a high-quality NDVI time-series data set based on the Savitzky-Golay filter. *Remote Sensing of Environment*, 91(3−4): 332−344. doi: 10.1016/j.rse.2004.03.014

Didan K, Huete A, 2006. MODIS vegetation index product series collection 5 change summary. Available at: http://landweb.nascom.nasa.gov/QAWWW/forPage/MOD13VIC5ChangesDocument062806.pdf.

Friedl M, Mciver D, Hodges J *et al*., 2002. Global land cover mapping from MODIS: Algorithms and early results. *Remote Sensing of Environment*, 83(1–2): 287–302. doi: 10.1016/S0034-4257(02)00078-0

Galford G, Mustard J, Melillo J *et al*., 2008. Wavelet analysis of MODIS time series to detect expansion and intensification of row-crop agriculture in Brazil. *Remote Sensing of Environment*, 112(5): 576–587. doi: 10.1016/j.rse.2007.05.017

Hird J, Mcdermid G, 2009. Noise reduction of NDVI time series: An empirical comparison of selected techniques. *Remote Sensing of Environment*, 113(1): 248–258. doi: 10.1016/j.rse.2008.09.003

Homer C, Huang C, Yang L *et al*., 2004. Development of a 2001 national land-cover database for the United States. *Photogrammetric Engineering and Remote Sensing*, 70(7): 829–840.

Huete A, Justice C, Leeuwen W V, 1999. MODIS vegetation index (MOD13) algorithm theoretical basis document (Version 3). Available at: http://modis.gsfc.nasa.gov/data/atbd/atbdmod13.pdf (accessed 20 March 2009).

Jönsson P, Eklundh L, 2002. Seasonality extraction by function-fitting to time series of satellite sensor data. *IEEE Transactions on Geoscience and Remote Sensing*, 40(8): 1824–1832. doi: 10.1109/TGRS.2002.802519

Julien Y, Sobrino J A, 2010. Comparison of cloud-reconstruction methods for time series of composite NDVI data. *Remote Sensing of Environment*, 114(3): 618–625. doi: 10.1016/j.rse.

2009.11.001

Liu C M, Yu J J, Kendy E, 2001. Groundwater exploitation and its impact on the environment in the North China Plain. *Water International*, 26(2): 265–272. doi: 10.1080/02508060108686913

Lobell D, Asner G, 2004. Cropland distributions from temporal unmixing of MODIS data. *Remote Sensing of Environment*, 93(3): 412–422. doi: 10.1016/j.rse.2004.08.002

Lotsch A, Tian Y, Friedl M *et al*., 2003. Land cover mapping in support of LAI and FPAR retrievals from EOS-MODIS and MISR: Classification methods and sensitivities to errors. *International Journal of Remote Sensing*, 24(10): 1997–2016. doi: 10.1080/01431160210154858

Lovell J L, Graetz R D, 2001. Filtering pathfinder AVHRR land NDVI data for Australia. *International Journal of Remote Sensing*, 22(13): 2649–2654. doi: 10.1080/01431160116874

Lu X, Liu R, Liu J *et al*., 2007. Removal of noise by wavelet method to generate high quality temporal data of terrestrial MODIS products. *Photogrammetric Engineering and Remote Sensing*, 73(10): 1129–1139.

Lunetta R, Knight J, Ediriwickrema J *et al*., 2006. Land-cover change detection using multi-temporal MODIS NDVI data. *Remote Sensing of Environment*, 105(2): 142–154. doi: 10.1016/j.rse.2006.06.018

Ma M, Veroustraete F, 2006. Reconstructing pathfinder AVHRR land NDVI time-series data for the Northwest of China. *Advances in Space Research*, 37(4): 835–840. doi: 10.1016/j.asr.2005.08.037

Mallat S, 1989. A theory for multiresolution signal decomposition: The wavelet representation. *IEEE Transactions on Pattern Analysis and Machine Intelligence*, 11(7): 674–693. doi: 10.1109/34.192463

Roerink G J, Menenti M, Verhoef W, 2000. Reconstructing cloud free NDVI composites using Fourier analysis of time series. *International Journal of Remote Sensing*, 21(9): 1911–1917. doi: 10.1080/014311600209814

Sakamoto T, Yokozawa M, Toritani H *et al*., 2005. A crop phenology detection method using time-series MODIS data. *Remote Sensing of Environment*, 96(3–4): 366–374. doi: 10.1016/j.rse.2005.03.008

Savitzky A, Golay M J E, 1964. Smoothing and differentiation of data by simplified least squares procedures. *Analytical Chemistry*, 36(8): 1627–1639. doi: 10.1021/ac60214a047

Sellers P, Tucker C, Collatz G *et al*., 1994. A global 1° by 1° NDVI data set for global studies. Part 2: The generation of global fields of terrestrial biophysical parameters from the NDVI. *International Journal of Remote Sensing*, 15(17): 3519–3545. doi: 10.1080/01431169408954343

Torrence C, Compo G, 1998. A practical guide to wavelet analysis. *Bulletin of the American Meteorological Society*, 79(1): 61–78.

USGS (U.S. Geological Survey), 2009. Land processes distributed active archive center (LP DAAC). Available at: https://lpdaac.usgs.gov/lpdaac/get_data/data_pool (accessed 20 March 2009).

Viovy N, Arino O, Belward A S, 1992. The best index slope extraction (BISE): A method for reducing noise in NDVI time-series. *International Journal of Remote Sensing*, 13(8): 1585–1590. doi: 10.1080/01431169208904212

Wardlow B, Egbert S, 2008. Large-area crop mapping using time-series MODIS 250 m NDVI data: An assessment for the US Central Great Plains. *Remote Sensing of Environment*, 112(3): 1096–1116. doi: 10.1016/j.rse.2007.07.019

Wardlow B, Egbert S, Kastens J, 2007. Analysis of time-series MODIS 250 m vegetation index data for crop classification in the US Central Great Plains. *Remote Sensing of Environment*, 108(3): 290–310. doi: 10.1016/j.rse.2006.11.021

Wessels K, Fries D R, Dempewolf J *et al*., 2004. Mapping regional land cover with MODIS data for biological conservation: Examples from the Greater Yellowstone Ecosystem, USA and Pará State, Brazil. *Remote Sensing of Environment*, 92(1): 67–83. doi: 10.1016/j.rse.2004.05.002

Wu G, De Leeuw J, Skidmore A *et al*., 2008. Comparison of MODIS and Landsat TM5 images for mapping tempo-spatial dynamics of Secchi disk depths in Poyang Lake National Nature Reserve, China. *International Journal of Remote Sensing*, 29(8): 2183–2198. doi: 10.1080/01431160701422254

Xiao X, Braswell B, Zhang Q *et al*., 2003. Sensitivity of vegetation indices to atmospheric aerosols: Continental-scale observations in Northern Asia. *Remote Sensing of Environment*, 84(3): 385–392. doi: 10.1016/S0034-4257(02)00129-3

Zhang M W, Zhou Q B, Chen Z X *et al*., 2008. Crop discrimination in Northern China with double cropping systems using Fourier analysis of time-series MODIS data. *International Journal of Applied Earth Observations and Geoinformation*, 10(4): 476–485. doi: 10.1016/j.jag.2007.11.002

Zhang X, Friedl M, Schaaf C *et al*., 2003. Monitoring vegetation phenology using MODIS. *Remote Sensing of Environment*, 84(3): 471–475. doi: 10.1016/S0034-4257(02)00135-9